UMSHA Press

AJDR
Avicenna Journal of Dental Research

Avicenna J Dent Res. 2025;17(2):70-78. doi:10.34172/ajdr.1969

http://ajdr.umsha.ac.ir

Original Article

Nanofibers Loaded With Vancomycin for the Treatment of Periodontal Infections: Synthesis, Characterization, Efficacy, and Safety Tests

Mahshad Noori Barkestani[1], Hazhir Maslahaty[1], Negar Sedghi Aminabad[2], Abolfazl Akbarzadeh[1], Mohammad Darvishi[3], Khayrolnesa Sadighi[4], Zahra Parhizgar[4*]

[1]Department of Periodontics, Faculty of Dentistry, Hamadan University of Medical Science, Hamadan, Iran
[2]Department of Medical Nanotechnology, Faculty of Advanced Medical Sciences, Tabriz University of Medical Sciences, Tabriz, Iran
[3]Department of Orthodontics, Faculty of Dentistry, Shahed University, Tehran, Iran
[4]Department of Periodontics, Mashhad University of Medical Science, Mashhad, Iran

Article history:
Received: August 6, 2024
Revised: September 29, 2024
Accepted: October 5, 2024
ePublished: June 30, 2025

***Corresponding author:**
Zahra Parhizgar,
Email: Parhizgar.zahra91@gmail.com

Abstract

Background: The primary function of periodontal wound dressing materials is to safeguard the wound site from microbial infections, regulate moisture levels, and administer bioactive chemicals. The present study aimed to create an antibiotic-loaded, interactive, bioactive nanofibrous. This scaffold will use polylactic glycolic acid loaded with vancomycin (Van) antibiotics.

Methods: The electrospinning approach was utilized to manufacture the dressing. In this study, nanofibers (NFs) were explored for the topical delivery of the antimicrobial drug Van, demonstrating their potential as a treatment alternative for periodontal infections. The Van-loaded NFs were created using an electrospinning technique, resulting in uniform, nanosized fibers (approximately 400 nm in diameter) with high drug entrapment efficiency and sustained release over 48 hours.

Results: In vitro, cytotoxicity tests using fibroblast cells confirmed the biocompatibility of the drug-loaded NFs. Additionally, in vitro, antibacterial tests revealed that the Van-loaded NFs maintained effective antibacterial activity against *Escherichia coli*, *Bacillus cereus*, *Salmonella typhimurium*, *Staphylococcus aureus*, and *Pseudomonas aeruginosa*. The additional characterization demonstrated that the synthesized NFs exhibit advantageous physicochemical features. Raising the antibiotic concentration diminished the tensile strength of NFs while enhancing the swelling properties. The release kinetics of the extract represented that approximately 80% of the drug was liberated from the NFs within 24 hours.

Conclusion: The MTT (3-[4,5-dimethylthiazol-2-yl]-2,5 diphenyl tetrazolium bromide), hemocompatibility, and antibacterial assays verified that the manufactured dressing was compatible with the living cells, killed the pathogenic bacteria, and stimulated the growth of fibroblast cells.

Keywords: Periodontal, Nanofibers, Vancomycin, Antibacterial

Please cite this article as follows: Noori Barkestani M, Maslahaty H, Sedghi Aminabad N, Akbarzadeh A, darvishi M, Sadighi K, et al. Nanofibers loaded with vancomycin for the treatment of periodontal infections: synthesis, characterization, efficacy, and safety tests. Avicenna J Dent Res. 2025;17(2):70-78. doi:10.34172/ajdr.1969

Background

Chronic periodontitis is an infectious inflammatory disease caused by bacteria in dental plaques. It destroys the supporting tissues of the teeth, including the gums, periodontal ligament, cementum, and alveolar bone, ultimately leading to tooth loss (1). Epidemiological studies indicate that 42% of 30–79-year-old adults (about 144 million people) in the United States have some form of periodontitis. Among them, 7.8% (approximately 4.7 million people) are affected by stage III or IV periodontitis, classified as grade B or C (2). Many of the local and systemic destructive effects of periodontitis are due to inflammation. The current theory suggests that periodontal inflammation arises from the interaction between the host immune system and a dysbiotic subgingival biofilm. Dysbiosis likely results from the

interplay among key potentially pathogenic microbes, with *Porphyromonas gingivalis* being the most prevalent periopathogen associated with chronic periodontitis. This bacterium is part of the so-called "red complex", which includes other significant pathogens in the disease (3). The complexity of periodontal infection therapy has arisen from the intricate mechanics of healing and the necessity to address non-clinical concerns, making wound care increasingly challenging (4-6). Overall, wound-healing physiology categorizes wounds into acute or chronic types. Acute wounds can occur when the body is exposed to strong forces such as shearing, blunting, or hitting, typically caused by heavy surfaces. Acute wounds may arise from explosions, fires, accidents, or exposure to corrosive chemicals or electricity. Generally, the vast majority of acute wounds undergo complete healing within around 8–12 weeks, leading to minimal formation of scars. Certain persistent injuries may require a recuperation period of up to 12 weeks. Ulcers arise due to chronic sickness, recurrent tissue injury, and postponed wound care. Factors such as anoxia, hypoxia, lesions, cell debris, and systemic barriers contribute to the formation of chronic wounds (7-10). Research has established a connection between the presence of moisture in the periodontal environment and the process of epithelialization, which refers to the growth of new skin cells, leading to faster overall wound healing. This is because the damp infected surface functions as a highly permeable membrane. Multiple effective drugs can be combined into the moisture at predetermined concentrations (11-13), providing the chance to comprehensively analyze any compounds generated during the wound-healing process and ascertain their rate of absorption and elimination. Moisture inhibits the inflammatory response, thus halting the course of harm. An atmosphere with conditions similar to an incubator, characterized by high levels of moisture, promotes the most effective healing process by facilitating rapid regeneration of tissues with minimal defects and scarring (14,15). The main purpose of an infected wound in periodontal is to accelerate the wound healing process while also protecting the spot. An optimal wound dressing should effectively sustain a warm and moist environment while also offering tailored functionalities according to the wound's attributes, including wound type, presence of infection, healing stage, and patient age (16-18).

Electrospinning, self-assembly, and phase separation are the primary techniques frequently employed to fabricate scaffolds for applications in biological engineering and drug delivery. Other techniques include frame synthesis, drawing, extraction, vapor phase polymerization, reaction kinetics-controlled solution synthesis, and chemical oxidative polymerization. Electrospinning is frequently regarded as the most extensively employed technology due to its straightforward operation and exceptional reproducibility (19,20). Some examples of biocompatible polymers include polyethylene oxide, polycaprolactone (PCL), polylactic acid, and polylactic-co-glycolic acid (PLGA). PLGA is particularly popular in biomedical applications due to its predictable degradation properties and ability to effectively interact with various biomolecules (21). Furthermore, it has poor solubility in water-based solvents, impeding its capacity to dissolve in the presence of the biological medium and other biocompatible polymers such as polyethylene oxide. Multiple research institutions have recently published data regarding the usage of PLGA in the domains of wound healing and drug delivery. According to previous research, PLGA nanofibers (NFs) have specific properties that make them useful for enhancing functionality in wound healing treatments. PLGA has several benefits in the synthesis of NFs, including biocompatibility, biodegradability, versatility, and controlled release. Biocompatibility implies that PLGA is well-tolerated in biological systems, making it ideal for medical applications. As regards biodegradability, PLGA gradually degrades in the body, which is advantageous for drug delivery and tissue engineering. Regarding versatility, the ratio of lactic to glycolic acid can be adjusted to tailor properties such as degradation rate and mechanical strength. In terms of controlled release, PLGA NFs can encapsulate drugs and provide sustained release, enhancing therapeutic effectiveness (22). Although PLGA has many advantages for NF synthesis, it has some limitations and weaknesses, such as hydrophilicity, mechanical properties, processing challenges, degradation products, limited drug loading capacity, and cost. This accelerates the process of tissue regeneration following injury. The incorporation of biomolecules into PLGA fibers is difficult because of their hydrophobic nature and the use of aqueous-based systems. Biomolecules experience decreased stability upon mixing, necessitating subsequent changes after spinning. Nevertheless, it is simpler to include antibiotics such as chloramphenicol, which hinders the activity of peptidyl transferase in the ribosome. Vancomycin (Van) is utilized for the treatment of bacterial infections (23). This study seeks to create a wound dressing with bioactive properties using electrospun NFs that contain Van.

Materials and Methods

Materials

The PLGA (85:15) was obtained from Birmingham Polymers, located near Pelham, Alabama. In addition, dimethylformamide (DMF), chloramphenicol, and all other chemicals, as well as the applied solvents, were purchased from Sigma-Aldrich Company (St. Louis, MO, USA). Moreover, the 3-(4,5-dimethylthiazol-2-yl)-2,5-diphenyl tetrazolium bromide (MTT) assay kit was obtained from Roth (Karlsruhe, Germany). Additionally, the fetal bovine serum, Dulbecco's Modified Eagle medium /F-12 cell culture media, trypsin-ethylenediaminetetraacetic acid, and penicillin-streptomycin (Pen-Strep) were purchased from Gibco (Karlsruhe, Germany). Unless specifically mentioned otherwise, all compounds were used in their original form

without any further purification. Finally, the L929 cell line was obtained from the Pasteur Institute in Iran, and the plastic and tissue culture plates were purchased from SPL Company (Korea).

Fabrication of the Periodontal Patch

Two concentrations of Van (10 mg/mL and 2 mg/mL) were dissolved in DMF. Next, 35 wt% PLGA was added to each combination, which had a molecular weight of 95 000 and a ratio of 85% lactic acid to 15% glycolic acid. The mixtures were combined overnight. Then, each solution was inserted into a 3-mL syringe and connected to the New Era NE-1000 syringe pump (Wantagh, NY). Subsequently, a voltage of 18 kV was delivered to the syringe's tip. In addition, the solution was applied to an aluminum foil collector using electrospinning for 30 minutes. Further, the solution was pumped at a rate of 8.5 mL per minute, maintaining a distance of 25 cm between the needle tip and the collector. The samples were placed in a vacuum overnight to ensure the full evaporation of any remaining DMF. The prepared polymeric solutions were converted to NFs via the applied voltage of 20 kV, a feeding rate of 0.5 mL/min, and a tip-to-collector distance of 10 cm.

Characterization of Fabricated Scaffolds

Scanning Electron Microscopy and Contact Angle

Before conducting microscopic examinations, the samples underwent a process of applying a thin layer of gold using a sputter-coating technique (SCD 004, Balzers, Germany). This is performed to enhance the surface's electrical conductivity and prevent the build-up of electric charge on the surface. The NF's morphology was examined using SEM (TESCAN VEGA3 XMU, 20 kV, Tescan, Brno, Czech Republic). Then, the scaffolds were analyzed using a static contact angle measurement apparatus (KRUSS, Hamburg, Germany) to determine the water contact angles of deionized water on three sections of each scaffold, and the average of these contact angles was calculated accordingly.

Porosity and Pore Size Measurement

The porosity and pore distribution in the scaffolds were assessed by analyzing SEM images with ImageJ software. To calculate the porosity, the total image area was divided by the surface area of the pores. This measurement was conducted on a series of SEM images, and the average results were recorded. Additionally, the average pore size and distribution were estimated by randomly measuring the size of at least 100 pores across various SEM images.

Swelling Behavior

The swelling properties of the fabricated scaffolds were evaluated using a method described in previous research (24). The original weight of each scaffold, with a diameter of 10 mm and a thickness of 5 mm, was measured. Subsequently, the scaffold was immersed in a phosphate-buffered saline (PBS) solution and subjected to incubation under controlled conditions at 37 ˚C. After removing any excess water from the surface of the scaffolds, the samples were weighed at defined time intervals. The swelling properties of the fabricated scaffolds were assessed using previous data (25). The scaffold swelling ratio was calculated using the following equation:

$$\text{Swelling ratio} = (Ww — Wd / Wd)$$

Ww and Wd denote the mass of the wet sample and the initial dry mass of the same sample, respectively. The mean ± standard deviation (SD) values were computed using data collected from three samples.

Degradation Assay

The in vitro degradation assay was conducted according to a previous study (24). Prior to initiating the hydrolytic degradation experiments, the samples were soaked in PBS for 2 hours to achieve swelling equilibrium. Afterward, the initial weight of the samples was recorded. The scaffolds were then placed in PBS (pH: 7.4) and maintained at 37 ˚C for 21 days, with 75.6% of the PBS solution replaced with fresh solution every 72 hours. At designated intervals, the samples were retrieved from the PBS, and their weights were measured. Wi and Wt represent the initial weight of the sample and the weight at various time points, respectively. The average values ± SD were calculated based on data from three scaffolds. Spectrophotometry was used to evaluate drug loading and the efficiency of Van entrapment in NFs. Specifically, 10 mg of dry NFs was dissolved in 1 mL of acetonitrile until the polymer was fully dissolved and the Van precipitated. The samples were centrifuged twice at 13 600 rpm for 20 minutes, and the absorbance of the resulting solution was measured at 282 nm. The scaffold degradation percentage was determined by the following equation:

$$\text{Degradation (\%)} = (Wt - Wi / Wi) \times 100$$

Hemolysis Induction Assay

The artificial NF-based scaffolds (50 mg) were subjected to 200 µL of freshly obtained and anticoagulated blood (diluted with PBS, at a ratio of 2:2.5) at 37 ˚C for 1 hour. Subsequently, the samples were subjected to centrifugation at a velocity of 1500 revolutions per minute for 3 minutes while maintaining a temperature of 40 ˚C. Finally, the instrument specifically intended for evaluating samples in microplates was used to measure the amount of light absorbed by the remaining liquid after centrifugation at a wavelength of 545 nm. The following equation was applied to calculate the hemolysis percentage:

$$\text{Hemolysis (\%)} = D_t - D_{nc} / D_{pc} - D_{nc} \times 100$$

D_t, D_{nc}, and D_{pc} correspond to the absorbance values of the sample, negative control, and positive control, respectively.

Cell Toxicity Analysis

The biocompatibility of the fabricated scaffolds was evaluated through in vitro cytotoxicity testing using the MTT assay. L929 cells were cultured in the RPMI medium supplemented with 10% fetal bovine serum and 1% penicillin/streptomycin. The cells were kept at 37 ˚C in a 5% CO_2 atmosphere. The scaffolds were cut into 1 mm thick and 6 mm diameter sections, with each piece weighing approximately 2.4 mg. The samples were sterilized using a two-step process (treatment with 70% ethanol, followed by 2 hours of UV exposure). Afterward, the specimens were washed twice with PBS and culture media. The scaffolds were then placed into a 48-well plate, and L929 cells were added at a density of 5×10^4 cells per scaffold. The culture medium was replaced every other day. The MTT solution (0.5 mg/mL) was added to each well at intervals of 3 days, 5 days, and 7 days and incubated at 37 ˚C for 4 hours. The liquid was then removed, and 150 µL of dimethyl sulfoxide was added to dissolve any insoluble formazan crystals. The plates were stirred in the dark for 15 minutes and then transferred to a 96-well plate. The absorbance of the formazan product was measured using a microplate spectrophotometer (Tecan's Sunrise, Austria) at 570 nm.

Bacterial Growth Inhibition Assays on Liquid Culture

Liquid cultures of *Escherichia coli*, *Bacillus cereus*, *Salmonella Typhimurium*, *Staphylococcus aureus*, and *Pseudomonas aeruginosa* were incubated overnight in tryptic soy broth at 37 ˚C. After 18 hours, 50 mL from each culture was transferred into test tubes containing 5 mL of sterile tryptic soy broth. The circular cutouts (12 mm in diameter) of Van-doped or undoped PLGA fibers were added to the test tubes prior to incubation. The cultures were then incubated for an additional 18 hours at 37 ˚C with shaking. Turbidity was assessed to determine bacterial growth (or inhibition) for each strain. In addition, optical absorbance measurements were taken to quantify growth inhibition. For this purpose, 100 µL from each culture was pipetted into a 96-well microplate, and absorbance at 600 nm was measured using a Tecan M-200 (Durham, NC) plate reader. The absorbance values from solutions with doped and undoped NFs were compared, with all experiments conducted in triplicate.

Statistical Analysis

Data were presented as mean ± standard deviation (mean ± SD) and analyzed using GraphPad Prism 9 software (San Diego, CA, USA). Statistical analyses were performed using one-way analysis of variance followed by post hoc Tukey's tests. A P value of less than 0.05 was considered statistically significant for all tests.

Results

Characterization of Nanofibers

The morphology of the manufactured NFs was assessed using the SEM imaging technique. Based on Figure 1, NFs had a structure that was organized in a straight line, with smooth outsides and connected cavities. It should be noted that the parameters of the electrospinning process have a significant impact on the morphology of electrospun NFs, which, in turn, determines their final physical and chemical properties.

The diameter of the manufactured NFs was measured by ImageJ software using the collected SEM images. The pure PLGA NFs had a diameter of 289 ± 48 nm, whereas the addition of Van led to the development of NFs with a larger diameter. The PLGA NF-loaded Van had a diameter of 371 ± 47 nm (Figure 2). Physical parameters such as temperature, pressure, and concentration of fiber can affect the morphology and diameter of NFs. Generally, increasing the temperatures decreases the viscosity of the molten material, leading to thinner and more uniform fibers. An increase in pressure usually compresses the material, potentially reducing fiber diameter and improving uniformity. An increase in concentration can increase viscosity, resulting in larger fiber diameters and more stress during processing, affecting morphology. These effects can vary depending on the material and production method (26).

The SEM imaging technique was employed to examine the surface morphology of the manufactured NFs (Figure 1). The results demonstrated that the manufactured NFs had a randomly oriented design with smooth surfaces and linked pores. The water contact angles were measured to assess the hydrophilicity of the generated dressing. Based on the results, including Van in PLGA NFs causes a decrease in water contact angles (Figure 3).

Permeability is one of the most important factors that determines the level of effectiveness of a biomaterial for skin regeneration. The electrospun nanofibrous meshes have a porous structure, which boosts cell adhesion, migration, and proliferation. Additionally, they can facilitate the exchange of gases and fluids and absorb exudates. During the process of wound healing and regeneration, this, in turn, acts as a catalyst for the formation of a new extracellular matrix (ECM). The liquid displacement method, based on Archimedes' principle, was utilized to determine the porosity of wound dressings. This technique is an indirect method that is employed to determine the pore size distribution of a membrane. The process begins with measuring a flux-pressure curve, followed by calculating the pore size distribution based on this information. The findings (Figure 4) demonstrated that the porosity of the created dressings was between 59% and 64%.

The loading efficacy of Van into the NFs was measured at around 32.01%. The swelling ratio of the electrospun nanofibrous meshes was assessed in a PBS solution at designated time intervals (Figure 5). All samples demonstrated substantial potential for swelling in terms of water absorption by dry scaffolds. After soaking for a long time, the swelling ratio dramatically increased, indicating

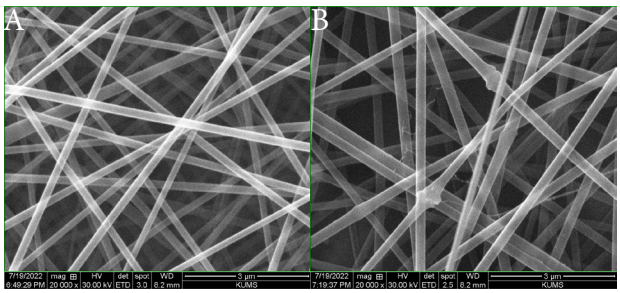

Figure 1. SEM Images of **(A)** PLGA and **(B)** PLGA-Van Nanofiber-Based Scaffolds. *Note.* SEM: Scanning electron microscopy; PLGA: Polylactic-co-glycolic acid; Van: Vancomycin

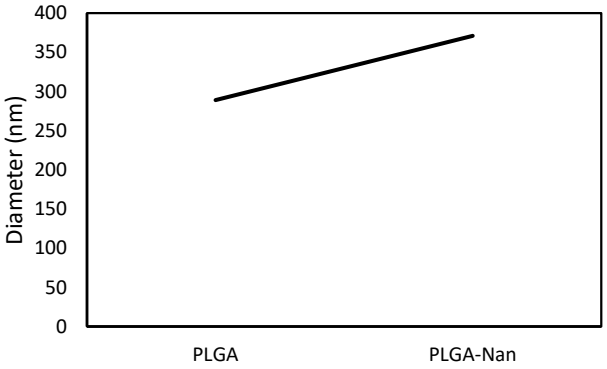

Figure 2. Diameter of Fabricated Nanofibers

a higher level of water absorption. Nevertheless, the scaffold ultimately reached a swelling equilibrium with a decrease in the rate of water absorption. The PLGA-Van NF represented a higher degree of edema compared to the PLGA-Van NF. The presence of the Van compound affected the rate of swelling in the samples, but the amount of reinforcement increased with a reduction in the swelling ratio. Therefore, the alterations in the porosity of the scaffolds and the corresponding decline in the polymer concentration within the scaffolds cause the swelling ratio to decrease with an increase in the concentration of Van. Moreover, the interaction between polymer components and water molecules primarily influences the swelling capacity of biopolymers.

The researchers studied the deliberate release of bioactive substances from electrospun NFs to the site of a wound to enhance wound healing and stimulate the regeneration of skin. An in vitro release study was performed to evaluate the capacity and efficacy of electrospun PLGA nanofibrous meshes in delivering a controlled release of Van. Based on the results (Figure 6), the Van loaded into the PLGA NFs exhibited a rapid release during the initial hours of the experiment.

Biological Evaluations

Hemocompatibility

Hemolysis assessments further indicated (Figure 7) that the fabricated NFs were compatible with blood (showing minimal hemolysis) and compatible with cells. Based on the findings, synthesized scaffolds can be used as scaffolds for wound healing.

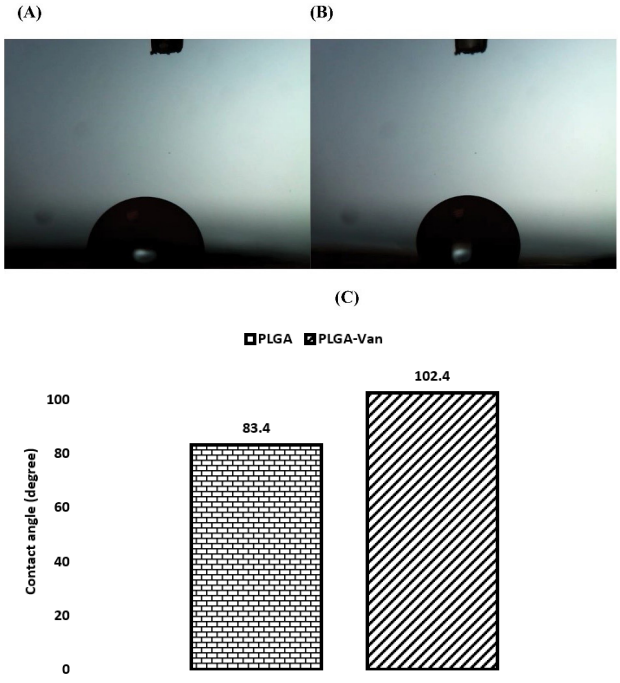

Figure 3. Surface Wettability of Fabricated Nanofibers: (A) PLGA, (B) PLGA-Van, and (C) Quantitative Results. *Note.* PLGA: Polylactic-co-glycolic acid; Van: Vancomycin

Cytotoxicity

When it comes to wound dressings, the ideal one should be biocompatible and capable of effectively performing its role without interfering with cellular processes that are involved in the healing process. Furthermore, these materials have been precisely developed to imitate the complicated three-dimensional organization of the ECM that is present in normal skin, allowing for the promotion of cell adhesion and proliferation. An in vitro MTT test assay was utilized to determine whether the electrospun PLGA nanofibrous meshes are biocompatible. Figure 8 illustrates the influence that these meshes have on the differentiation of L-929 cells. When cells were exposed to both the unloaded and Van-loaded PLGA nanofibrous mesh mats, there was no evident detrimental effect on the survival of the cells. The results demonstrated that none of the scaffolds exhibited any toxicity when compared to the control group of two-dimensional grown cells after 3 days, 5 days, and 7 days.

Antibacterial Activity

After overnight incubation, the bacterial cultures exposed to Van-loaded fibers were assessed for turbidity (or lack of turbidity) to indicate growth inhibition due to Van release into the media. Optical absorbance measurements were performed to quantify these results. All five solutions containing PLGA-Van fibers represented reduced absorbance compared to the same bacterial solutions with PLGA fibers. Figure 9 depicts the absorbance values and percentage of growth inhibition calculated from the normalized absorbance differences between solutions with PLGA-Van NFs and PLGA fibers. Three separate experiments were conducted, and the average absorbance

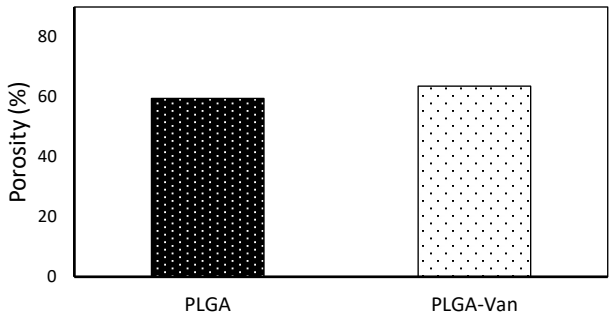

Figure 4. The Porosity of the Dressings, Measured Based on Archimedes' Principle-Based Liquid Displacement

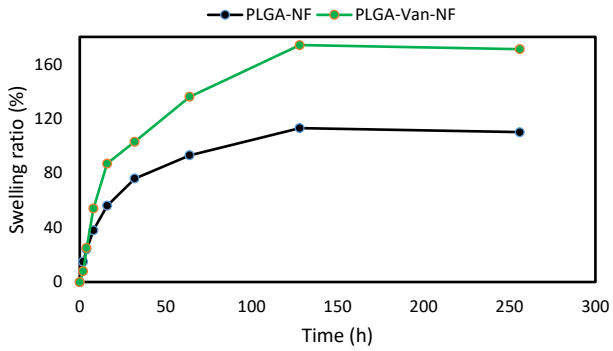

Figure 5. Swelling Value of Dressings

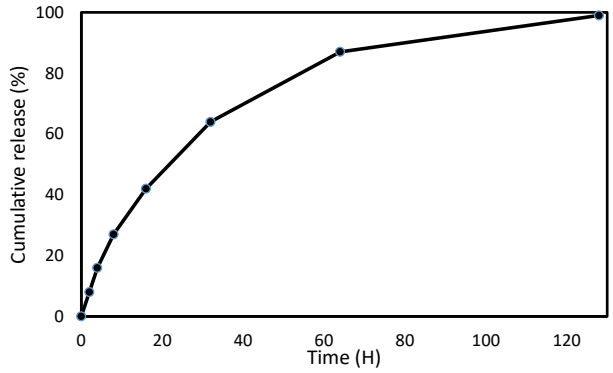

Figure 6. The Release Profile of the Loaded Van From the PLGA NF. Note. PLGA: Polylactic-co-glycolic acid; Van: Vancomycin; NF: Nanofiber

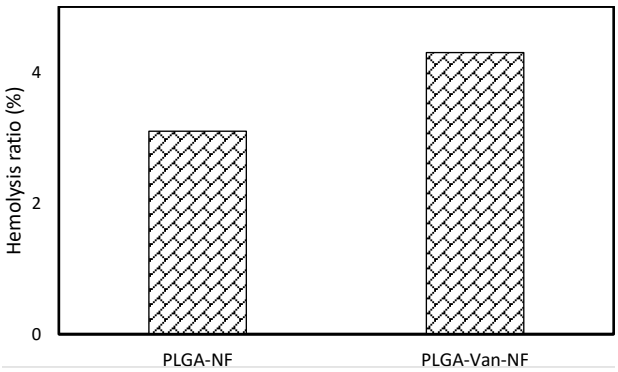

Figure 7. Hemolysis Value of the Periodontal Patch

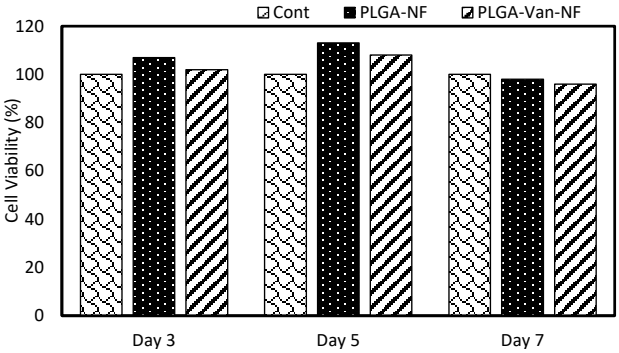

Figure 8. Viability of L929 Fibroblast Cells Under Incubation With the Wound Dressings Measured by the MTT Assay. *Note*. MTT: 3-(4,5-dimethylthiazol-2-yl)-2,5-diphenyl tetrazolium bromide

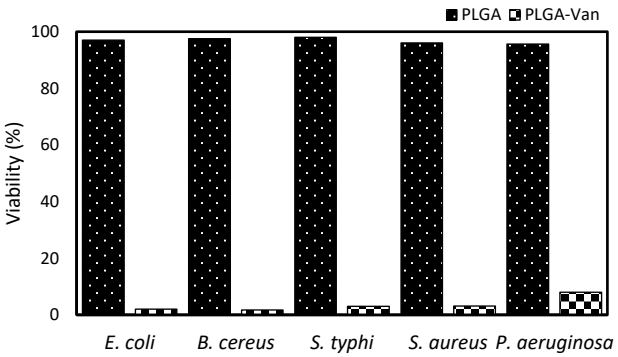

Figure 9. Bacterial Growth Inhibition by Vancomycin-Loaded Nanofibers in Liquid Culture. *Note*. PLGA: Polylactic-co-glycolic acid; TSB: Tryptic soy broth; NF: Nanofibers; Van: Vancomycin. Van-loaded NFs were placed in 5 mL TSB and inoculated with bacterial cultures. Absorbance (600 nm) values were measured for samples containing Van-loaded PLGA NFs and unmodified PLGA NFs. Growth inhibition is reported as the percentage difference between absorbance values for loaded and unloaded NFs

values are displayed in Figure 9. The data revealed that the growth of *E. coli*, *B. cereus*, and *S. typhimurium* was significantly inhibited by the presence of Van-loaded NFs, while that of *S. aureus* and *P. aeruginosa* was inhibited to a lesser extent. The average percentage of growth inhibition for *E. coli*, *B. cereus*, *S. typhimurium*, *S. aureus*, and *P. aeruginosa* was 95.2%, 93.2%, 94.3%, 56.2%, and 41.9%, respectively.

Discussion

Our findings corroborate those of the study by Suryamathi et al, which demonstrated that the inclusion of the *Tridax procumbens* extract increased the mean diameter of PCL NFs (27). In a separate investigation, researchers found that the inclusion of the *Inula graveolens* (L.) extract in PLGA NFs led to an augmentation in the diameter of NFs (28), which is in line with the results of a similar study. Other studies have reported contradictory results, indicating that the inclusion of antibiotics leads to a reduction in the diameter of NFs. A study has shown that the addition of *Chelidonium majus* L. to a solution of PCL/polyvinyl (PVA)/pectin (PEC) polymers resulted in the reduction of NF thickness (29). Motealleh et al found that the inclusion of chamomile in NFs made of PLGA/polystyrene (65/35) by utilizing the electrospinning technique produced a comparable outcome. In a previous study, the researchers observed a reduction in the average dimensions of NFs, specifically from 268 nm to

175 nm, following the inclusion of chamomile (30). The authors suggested that the decrease in the diameter of NFs, after incorporating the extract, may be attributed to a decrease in the viscosity of the polymeric solution. Furthermore, their morphological attributes closely resemble the collagen fibers present in the natural ECM, exhibiting dimensions that vary between 50 nm and 500 nm. They possess the capacity to enhance cell adhesion and proliferation, restrict fluid accumulation, and enhance the diffusion of moisture vapor. This ultimately promotes an effective periodontal wound-healing process (31-33). The parameters of the electrospinning process primarily govern the morphology of electrospun NFs, hence determining their ultimate physical and chemical properties (29). An optimal wound dressing should possess hydrophilic properties to effectively absorb wound exudates and maintain a moist wound environment.

The findings of a study conducted by Agnes Mary et al revealed that the incorporation of aloe vera into PCL NFs led to a reduction in mechanical strength (34). Likewise, a different investigation reported that the incorporation of *Chelidonium majus* L. into PCL/PVA-PEC NFs could decrease their mechanical strength. The water absorption capacity of tissue engineering scaffolds is essential as it governs the ability of biological solutions to be soaked up, nutrients to permeate, and metabolic waste to be delivered within the biomaterials (35). The expandability of biomaterials is vital for their use in wound healing since it enables them to absorb excessive exudate, which is mostly generated during the inflammatory phase of the healing process. This is because it allows them to absorb larger amounts of exudates. Effective absorption of wound exudates is crucial for preventing adverse outcomes, such as impeding cell adhesion and migration, excessive moisture accumulation in the surrounding tissue, and bacterial penetration, all of which can result in wound infections (36).

Periodontal wound dressings can display cytotoxic and genotoxic characteristics, perhaps resulting in the emergence of bacterial resistance to these substances. Additionally, wound dressings have the potential to interact with blood cells that have an unfavorable surface charge, leading to the loss of red blood cells (hemolysis) due to their exceedingly small size. The influence of hemolysis on the process of wound healing is widely recognized. Free hemoglobin, generated by damaged red blood cells, can inactivate active nitric oxide, which is essential for vascularization, thus leading to a prolonged healing duration. Additionally, free hemoglobin can obstruct the growth of fibroblasts and hamper the process of collagen remodeling (37-40). Based on the results, none of the scaffolds showed toxicity in comparison to the control group of cells grown in a two-dimensional manner after 3 days, 5 days, and 7 days. Furthermore, the PLGA-Van demonstrated significantly higher cell viability compared to the control group at both the 3-day and 5-day intervals. Accordingly, the composition of the scaffolds has a substantial impact on their biocompatibility characteristics. The United States Food and Drug Administration has approved the use of PLGA as a biomaterial (41). The results of the Student's T-test confirmed a significant difference in growth between negative controls (PLGA NFs) and Van-loaded PLGA NFs at a 95% confidence interval for *E. coli*, *B. cereus*, and *S. typhimurium*. The research revealed that the disparity in growth suppression between loaded and free NFs was less pronounced for *S. aureus* and *P. aeruginosa* but remained statistically significant at the 90% confidence level.

Conclusion

The incorporation of antibacterial compounds into the production of polymeric electrospun NFs has been recognized as a viable method to enhance the effectiveness and efficiency of wound dressings with antibacterial properties. The present study successfully included Van, a substance renowned for its ability to enhance antibacterial activity and promote wound healing, into electrospun PLGA nanofibrous wound dressings using the electrospinning process for the first time. A comprehensive examination was performed on the dressing materials to determine their morphological, chemical, physical, and biological characteristics. The PLGA/Van nanofibrous meshes, which were created artificially, displayed a morphology that closely resembled the structure of the ECM found in actual skin. They exhibited the ability to maintain a damp environment at the site of the wound. Furthermore, the in vitro release experiment demonstrated that Van, which was integrated into the NF structure, was consistently discharged into the medium over 48 hours. The PLGA NFs coated with Van represented stimulatory actions, rendering the produced dressing very suitable for wound healing purposes.

Acknowledgments

The researchers of this study are grateful to Hamadan University of Medical Sciences for their financial support in conducting research.

Authors' Contribution

Mahshad Noori Barkestani, Abolfazl Akbarzadeh, and Hazhir Maslahaty designed the study. In addition, Mohammad darvishi contributed to conducting experimental studies and drafting the work. Further, Negar Sedghi Aminabad performed the tests and collected and analyzed the data. Furthermore, Zahra Parhizgar wrote and edited the manuscript. All authors read and approved the final manuscript.

Competing Interests

The authors declare that there is no potential conflict of interests in the present study.

Data Availability Statement

The authors confirm that the data supporting the findings of this study are available within the article.

Ethical Approval

The protocol of this in vitro study was approved by the Ethics Committee of Mashhad University of Medical Sciences.

Funding

The study was supported by a grant from the Vice-Chancellor for Research at Mashhad University of Medical Sciences.

References

1. Jönsson B, Abrahamsson KH. Overcoming behavioral obstacles to prevent periodontal disease: behavioral change techniques and self-performed periodontal infection control. Periodontol 2000. 2020;84(1):134-44. doi: 10.1111/prd.12334.
2. Shah PD, Badner VM, Moss KL. Association between asthma and periodontitis in the US adult population: a population-based observational epidemiological study. J Clin Periodontol. 2022;49(3):230-9. doi: 10.1111/jcpe.13579.
3. Mei F, Xie M, Huang X, Long Y, Lu X, Wang X, et al. *Porphyromonas gingivalis* and its systemic impact: current status. Pathogens. 2020;9(11):944. doi: 10.3390/pathogens9110944.
4. Boateng J, Catanzano O. Advanced therapeutic dressings for effective wound healing--a review. J Pharm Sci. 2015;104(11):3653-80. doi: 10.1002/jps.24610.
5. Frykberg RG, Banks J. Challenges in the treatment of chronic wounds. Adv Wound Care (New Rochelle). 2015;4(9):560-82. doi: 10.1089/wound.2015.0635.
6. Pereira RF, Bártolo PJ. Traditional therapies for skin wound healing. Adv Wound Care (New Rochelle). 2016;5(5):208-29. doi: 10.1089/wound.2013.0506.
7. Whitney JD. Overview: acute and chronic wounds. Nurs Clin North Am. 2005;40(2):191-205. doi: 10.1016/j.cnur.2004.09.002.
8. Falanga V, Isseroff RR, Soulika AM, Romanelli M, Margolis D, Kapp S, et al. Chronic wounds. Nat Rev Dis Primers. 2022;8(1):50. doi: 10.1038/s41572-022-00377-3.
9. Dai C, Shih S, Khachemoune A. Skin substitutes for acute and chronic wound healing: an updated review. J Dermatolog Treat. 2020;31(6):639-48. doi: 10.1080/09546634.2018.1530443.
10. Sharifi E, Sadati SA, Yousefiasl S, Sartorius R, Zafari M, Rezakhani L, et al. Cell loaded hydrogel containing Ag-doped bioactive glass-ceramic nanoparticles as skin substitute: Antibacterial properties, immune response, and scarless cutaneous wound regeneration. Bioeng Transl Med. 2022;7(3):e10386. doi: 10.1002/btm2.10386.
11. Junker JP, Kamel RA, Caterson EJ, Eriksson E. Clinical impact upon wound healing and inflammation in moist, wet, and dry environments. Adv Wound Care (New Rochelle). 2013;2(7):348-56. doi: 10.1089/wound.2012.0412.
12. Atiyeh BS, Ioannovich J, Al-Amm CA, El-Musa KA. Management of acute and chronic open wounds: the importance of moist environment in optimal wound healing. Curr Pharm Biotechnol. 2002;3(3):179-95. doi: 10.2174/1389201023378283.
13. Field FK, Kerstein MD. Overview of wound healing in a moist environment. Am J Surg. 1994;167(1A):2S-6S. doi: 10.1016/0002-9610(94)90002-7.
14. Kharaziha M, Baidya A, Annabi N. Rational design of immunomodulatory hydrogels for chronic wound healing. Adv Mater. 2021;33(39):e2100176. doi: 10.1002/adma.202100176.
15. Chhabra S, Chhabra N, Kaur A, Gupta N. Wound healing concepts in clinical practice of OMFS. J Maxillofac Oral Surg. 2017;16(4):403-23. doi: 10.1007/s12663-016-0880-z.
16. Liang Y, He J, Guo B. Functional hydrogels as wound dressing to enhance wound healing. ACS Nano. 2021;15(8):12687-722. doi: 10.1021/acsnano.1c04206.
17. Boateng JS, Matthews KH, Stevens HN, Eccleston GM. Wound healing dressings and drug delivery systems: a review. J Pharm Sci. 2008;97(8):2892-923. doi: 10.1002/jps.21210.
18. O'Callaghan S, Galvin P, O'Mahony C, Moore Z, Derwin R. 'Smart' wound dressings for advanced wound care: a review. J Wound Care. 2020;29(7):394-406. doi: 10.12968/jowc.2020.29.7.394.
19. Li Y, Zhu J, Cheng H, Li G, Cho H, Jiang M, et al. Developments of advanced electrospinning techniques: a critical review. Adv Mater Technol. 2021;6(11):2100410. doi: 10.1002/admt.202100410.
20. Agarwal S, Wendorff JH, Greiner A. Use of electrospinning technique for biomedical applications. Polymer. 2008;49(26):5603-21. doi: 10.1016/j.polymer.2008.09.014.
21. Javid-Naderi MJ, Behravan J, Karimi-Hajishohreh N, Toosi S. Synthetic polymers as bone engineering scaffold. Polym Adv Technol. 2023;34(7):2083-96. doi: 10.1002/pat.6046.
22. Soscia DA, Raof NA, Xie Y, Cady NC, Gadre AP. Antibiotic-loaded PLGA nanofibers for wound healing applications. Adv Eng Mater. 2010;12(4):B83-8. doi: 10.1002/adem.200980016.
23. Battista S, Allegritti E, Marconi C, Bellio P, Galantini L, Del Giudice A, et al. Influence of lipid composition on physicochemical and antibacterial properties of vancomycin-loaded nanoscale liposomes. ACS Appl Nano Mater. 2024;7(1):1348-56. doi: 10.1021/acsanm.3c05419.
24. Echave MC, Erezuma I, Golafshan N, Castilho M, Kadumudi FB, Pimenta-Lopes C, et al. Bioinspired gelatin/bioceramic composites loaded with bone morphogenetic protein-2 (BMP-2) promote osteoporotic bone repair. Biomater Adv. 2022;134:112539. doi: 10.1016/j.msec.2021.112539.
25. Ebrahimvand Dibazar Z, Mohammadpour M, Samadian H, Zare S, Azizi M, Hamidi M, Azizi M, et al. Bacterial polyglucuronic acid/alginate/carbon nanofibers hydrogel nanocomposite as a potential scaffold for bone tissue engineering. Materials. 2022;15(7):2494. doi: 10.3390/ma15072494.
26. Deitzel JM, Kleinmeyer J, Harris D, Beck Tan NC. The effect of processing variables on the morphology of electrospun nanofibers and textiles. Polymer. 2001;42(1):261-72. doi: 10.1016/S0032-3861(00)00250-0.
27. Suryamathi M, Ruba C, Viswanathamurthi P, Balasubramanian V, Perumal P. *Tridax procumbens* extract loaded electrospun PCL nanofibers: a novel wound dressing material. Macromol Res. 2019;27(1):55-60. doi: 10.1007/s13233-019-7022-7.
28. Al-Kaabi WJ, Albukhaty S, Al-Fartosy AJ, Al-Karagoly HK, Al-Musawi S, Sulaiman GM, et al. Development of *Inula graveolens* (L.) plant extract electrospun/polycaprolactone nanofibers: a novel material for biomedical application. Appl Sci. 2021;11(2):828. doi: 10.3390/app11020828.
29. Mouro C, Gomes AP, Ahonen M, Fangueiro R, Gouveia IC. *Chelidonium majus* L. incorporated emulsion electrospun PCL/PVA_PEC nanofibrous meshes for antibacterial wound dressing applications. Nanomaterials (Basel). 2021;11(7):1785. doi: 10.3390/nano11071785.
30. Motealleh B, Zahedi P, Rezaeian I, Moghimi M, Abdolghaffari AH, Zarandi MA. Morphology, drug release, antibacterial, cell proliferation, and histology studies of chamomile-loaded wound dressing mats based on electrospun nanofibrous poly(ε-caprolactone)/polystyrene blends. J Biomed Mater Res B Appl Biomater. 2014;102(5):977-87. doi: 10.1002/jbm.b.33078.
31. Juncos Bombin AD, Dunne NJ, McCarthy HO. Electrospinning of natural polymers for the production of nanofibres for wound healing applications. Mater Sci Eng C Mater Biol Appl. 2020;114:110994. doi: 10.1016/j.msec.2020.110994.
32. Safdari M, Shakiba E, Kiaie SH, Fattahi A. Preparation and characterization of ceftazidime loaded electrospun silk fibroin/gelatin mat for wound dressing. Fibers Polym. 2016;17(5):744-50. doi: 10.1007/s12221-016-5822-3.
33. Pedram Rad Z, Mokhtari J, Abbasi M. Fabrication and characterization of PCL/Zein/Gum arabic electrospun nanocomposite scaffold for skin tissue engineering. Mater Sci Eng C Mater Biol Appl. 2018;93:356-66. doi: 10.1016/j.

msec.2018.08.010.
34. Agnes Mary S, Giri Dev VR. Electrospun herbal nanofibrous wound dressings for skin tissue engineering. The Journal of The Textile Institute. 2015;106(8):886-95. doi: 10.1080/00405000.2014.951247.
35. Liu M, Dai L, Shi H, Xiong S, Zhou C. In vitro evaluation of alginate/halloysite nanotube composite scaffolds for tissue engineering. Mater Sci Eng C Mater Biol Appl. 2015;49:700-12. doi: 10.1016/j.msec.2015.01.037.
36. Negut I, Dorcioman G, Grumezescu V. Scaffolds for wound healing applications. Polymers (Basel). 2020;12(9):2010. doi: 10.3390/polym12092010.
37. Jensen FB. The dual roles of red blood cells in tissue oxygen delivery: oxygen carriers and regulators of local blood flow. J Exp Biol. 2009;212(Pt 21):3387-93. doi: 10.1242/jeb.023697.
38. Bernatchez SF, Menon V, Stoffel J, Walters SA, Lindroos WE, Crossland MC, et al. Nitric oxide levels in wound fluid may reflect the healing trajectory. Wound Repair Regen. 2013;21(3):410-7. doi: 10.1111/wrr.12048.
39. Herold S, Exner M, Nauser T. Kinetic and mechanistic studies of the NO*-mediated oxidation of oxymyoglobin and oxyhemoglobin. Biochemistry. 2001;40(11):3385-95. doi: 10.1021/bi002407m.
40. Harrison SL, Vavken P, Murray MM. Erythrocytes inhibit ligament fibroblast proliferation in a collagen scaffold. J Orthop Res. 2011;29(9):1361-6. doi: 10.1002/jor.21321.
41. Gentile P, Chiono V, Carmagnola I, Hatton PV. An overview of poly(lactic-co-glycolic) acid (PLGA)-based biomaterials for bone tissue engineering. Int J Mol Sci. 2014;15(3):3640-59. doi: 10.3390/ijms15033640.